Research paper

Struct Multidisc Optim 26, 308–317 (2004)
DOI 10.1007/s00158-003-0351-2

An integrated approach to topology, sizing, and shape optimization*

M. Zhou, N. Pagaldipti, H.L. Thomas, Y.K. Shyy

Abstract Topology optimization has become very popular in industrial applications, and most FEM codes have implemented certain capabilities of topology optimization. However, most codes do not allow simultaneous treatment of sizing and shape optimization during the topology optimization phase. This poses a limitation on the design space and therefore prevents finding possible better designs since the interaction of sizing and shape variables with topology modification is excluded. In this paper, an integrated approach is developed to provide the user with the freedom of combining sizing, shape, and topology optimization in a single process.

Key words structural optimization, topology optimization, shape optimization, sizing, optimization software

1 Introduction

Sizing, shape, and topology optimization are the major ingredients of the technology of structural optimization. Sizing and shape optimization capabilities have been available since the late 1980s in popular FEM software applications such as MSC/NASTRAN (MSC Software 1999) and ANSYS (1999). Specialized structural optimization software such as GENESIS (VMA Engineering 1999) also emerged subsequently, utilizing more advanced approximation technology for enhancing overall efficiency. This development has led to a steady increase in industrial application of optimization technology in the past decade. A notable phenomenon seen in recent years is the fast growth of the application of topology optimization, especially in the automobile industry, largely owing to its significant impact in creating more efficient design concepts at the preliminary design stage. Existing structural optimization software applications mentioned above have added some basic topology optimization capabilities as a complementary tool to their existing sizing and shape optimization capabilities. At the same time, special topology optimization codes such as Altair OptiStruct (Altair Engineering 1999) have also appeared in this fast-growing field. In general, specialized optimization codes, although equipped with fewer analysis capabilities than general FEM codes, offer more features and higher efficiency for optimization. The reasons for this are twofold: (1) highly specialized codes are typically smaller and therefore more flexible for incorporating the latest developments than general codes, and (2) for specialized codes, highest priority is devoted to its core technology of optimization.

To date, topology optimization has been performed separately while sizing and shape optimization can be combined into a single process. This separation of topology optimization may be due to the fact that it is usually used as a tool for finding efficient design concepts at the early design stage, whereas sizing and shape optimization are tools for detailed design at a later stage. However, feedback from industrial users have shown that, even at the stage of conceptual study, it may be desirable to consider the interaction of some key sizing and shape parameters with topology optimization. For example, one might want to optimize the thickness of a base plate and simultaneously try to locate stiffening ribs using topology optimization. Also, the contour shape of the plate may be optimized as well during the optimization of the rib pattern. For such design problems, an integrated approach not only allows the freedom of finding better designs by taking into account the interaction of sizing, shape, and topology variables, but it also helps achieve this goal more efficiently within a single iterative process.

In this paper, this integrated optimization problem is mathematically formulated in a general fashion, which

Received: 24 January 2002
Revised manuscript received: 26 May 2003
Published online: 23 December 2003

M. Zhou✉, N. Pagaldipti, H.L. Thomas, Y.K. Shyy

Altair Engineering, Inc., 2445 MacCabe Way, Suite 100, Irvine, CA 92614, USA
e-mail: zhou@altair.com

* Extended version of a paper presented at the 8th AIAA/ISSMO MAO conference, held in Long Beach, CA, 2000

allows the consideration of multiple constraints involving all types of responses. Owing to the large number of design variables, local constraints such as stress constraints are not considered for structural parts that involve topological design variables. Advanced approximation techniques based on intermediate responses and intermediate variables are applied in the implementation of the iterative process. To further enhance the efficiency of the design process, the approximation formulation of the intermediate responses corresponding to a specific constraint or the objective function are adapted based on the iteration history among linear, reciprocal, and convex approximations. Another key objective of this work is to provide an assessment of state-of-the-art advanced approximation technologies and create a highly efficient implementation within the commercial structural optimization code Altair OptiStruct. While OptiStruct has been a specialized product for topology optimization only, this development extends it into a general structural optimization tool with the unique feature of allowing users to combine sizing and shape optimization with topology optimization.

2 Optimization problem

The general optimization problem can be stated mathematically as follows:

$$\begin{aligned} &\text{Minimize} \quad f(\mathbf{X}) \\ &\text{Subject to} \quad g_j(\mathbf{X}) - g_j^U \leqslant 0\,, \quad j = 1, \ldots, M \\ &\qquad\qquad x_i^L \leq x_i \leq x_i^U\,, \quad i = 1, \ldots, N, \end{aligned} \tag{1}$$

where $f(\mathbf{X})$ represents the objective function, $g_j(\mathbf{X})$ and g_j^U represent the j-th constraint response and its upper bound, respectively, M is the total number of constraints, x_i is the i-th design variable, and x_i^L and x_i^U represent its lower and upper bounds, respectively. The total number of design variables is N. In the problem considered in this paper, the design variables include: (1) sizing variables that define the cross-sectional dimensions of 1-D elements (rods and beams) and 2-D elements (plates and shells); (2) shape variables that define the shape variation of existing boundaries; and (3) topology variables that define the generalized material distribution allowing topological changes to the structure. The objective function and design constraints can be any of the following responses: volumes or weights of structural parts, compliance, eigenfrequencies, displacements, and stresses. An equation utility has also been developed that allows users to formulate any custom response using the supported responses and design variables (Altair Engineering 1999). Owing to numerical difficulties, stress constraints could not be applied to the structural domain for topology optimization.

Shape variations in this work are defined as a linear combination of predefined vectors of shape perturbation:

$$\mathbf{Z}(\mathbf{X}) = \mathbf{Z}_0 + \sum_{i=1}^{K} x_i \mathbf{PV}_i, \tag{2}$$

where $\mathbf{Z}$ is the vector of nodal coordinates, $\mathbf{Z}_0$ is the vector of nodal coordinates at the initial design, $\mathbf{PV}_i$ is the i-th grid perturbation vector, and K is the total number of shape design variables. Note that the vector $\mathbf{Z}$ must also include internal nodes of the finite element mesh in order to avoid mesh distortion. This approach is easy to implement since it needs neither remeshing capability nor a mesh smoothing algorithm during the iterative process. However, it may encounter mesh distortion for large shape changes. The literature on shape optimization is very extensive, and reviews can be found in survey articles and some recent papers (see, e.g., Haftka and Grandhi 1986; Ding 1986; Kikuchi *et al.* 1986; Chang and Choi 1992; Yang *et al.* 1992; Schramm and Pilkey 1993; Schleupen *et al.* 1995). An overview of sizing optimization can be found in textbooks and review articles (see, e.g., Schmit 1981; Vanderplaats 1982; Haftka and Gürdal 1992; Kirsch 1993).

Topology design variables are parameters of microstructures in the homogenization approach (Bendsøe and Kikuchi 1988; Allaire and Kohn 1993; and Olhoff *et al.* 1998) or the material density ρ_i of each element in the density approach termed SIMP (Bendsøe 1989; Zhou and Rozvany 1991). An overview of topology optimization can be found in the book by Bendsøe (1995) and the review article by Rozvany *et al.* (1995). To achieve a 0/1 density distribution, the following power law penalization is used for the density approach

$$\bar{\mathbf{K}}_i(\rho) = \rho_i^p \mathbf{K}_i, \tag{3}$$

where $\bar{\mathbf{K}}_i$ and $\mathbf{K}_i$ represent the penalized and nonpenalized stiffness matrices, respectively. The parameter p is the penalization factor, which typically takes values between 2 and 4. Special numerical difficulties associated with topology optimization such as checkerboarding and mesh dependency have been addressed in the literature (for an overview see Sigmund and Petersson 1998). An efficient approach to checkerboard and minimum member size control has been developed and implemented recently by Zhou *et al.* (2001) in Altair OptiStruct (Altair Engineering 1999). This technique highly enhances the manufacturability of solutions.

3 Approximation formulations

The general approach to the optimization problem in Eq. 1 is the approximation concept approach pioneered by Schmit and Farshi (1974). In this approach, the optimization problem is solved by solving a series of explicit approximate problems. The overall efficiency of

this approach is determined by the accuracy of the approximation. Typical approximation formulations used in structural optimization are linear approximation shown in Eq. 4, reciprocal approximation in Eq. 5 (Schmit and Farshi 1974), and convex approximation in Eq. 6 (Haftka and Starnes 1976):

$$\tilde{g}_j(\mathbf{X}) = g_{j0} + \sum_{i=1}^{N} \frac{\partial g_j}{\partial x_i}(x_i - x_{i0}) \tag{4}$$

$$\tilde{g}_j(\mathbf{X}) = g_{j0} - \sum_{i=1}^{N} \frac{\partial g_j}{\partial x_i} x_{i0}^2 \left(\frac{1}{x_i} - \frac{1}{x_{i0}}\right) \tag{5}$$

$$\tilde{g}_j(\mathbf{X}) = g_{j0} + \sum_{i=1}^{N} \frac{\partial g_j}{\partial x_i} c_{ji}(x_i - x_{i0})$$

$$\text{with } c_{ji} = 1 \quad \text{if } \frac{\partial g_j}{\partial x_i} \geq 0\,; \quad c_{ji} = \frac{x_{i0}}{x_i} \quad \text{if } \frac{\partial g_j}{\partial x_i} < 0. \tag{6}$$

The formulation in terms of mixed variables in Eq. 6 is also termed conservative approximation since it has been shown by Haftka and Starnes (1976) that this formulation gives a more conservative approximation of the constraint compared with both linear and reciprocal approximations. Because this approximation is convex and separable, it is used to create an efficient dual method by Fleury and Braibant (1986).

Advanced approximation techniques developed in the late 1980s utilize the use of intermediate variables and intermediate responses to enhance the quality of approximation (Vanderplaats and Salajegheh 1989; Zhou 1989; Canfield 1990; Zhou and Xia 1990; Vanderplaats and Thomas 1993; Zhou and Thomas 1993). For sizing problems, the intermediate variables are the following cross-sectional properties:

$$\mathbf{Y}_i = (A, I1, I2, J, NSM)_i^T \quad \text{for beams}$$
$$\mathbf{Y}_i = (t, D, t_s, NSM)_i^T \quad \text{for shells,}$$

where A is the cross-sectional area, and $I1$, $I2$, and J are moments of inertia of the i-th beam properties. *NSM* stands for nonstructural mass. t, D, and t_s are, respectively, the thickness, bending stiffness, and shear thickness of the i-th shell properties. The above intermediate variables $\mathbf{Y}$ can be explicitly expressed as functions of sizing variables $\mathbf{X}$, i.e., $\mathbf{Y} = \mathbf{Y}(\mathbf{X})$. The quality of the approximation of displacements has been shown to be highly enhanced when reciprocal approximation is formulated in terms of intermediate variables $\mathbf{Y}$:

$$\tilde{g}_j(\mathbf{X}) = \tilde{g}_j(\mathbf{Y}(\mathbf{X})) = g_{j0} - \sum_{i=1}^{N} \frac{\partial g_j}{\partial y_i} y_{i0}^2 \left(\frac{1}{y_i} - \frac{1}{y_{i0}}\right). \tag{7}$$

It can be shown that the above approximation is exact for statically determinate structures. For stress constraints, the relevant element forces, termed intermediate responses herein, are approximated as follows:

$$\tilde{\mathbf{F}}_k(\mathbf{X}) = \tilde{\mathbf{F}}_k(\mathbf{Y}(\mathbf{X})) = F_{k0} + \sum_{i=1}^{N} \frac{\partial F_k}{\partial y_i}(y_i - y_{i0}). \tag{8}$$

Then the approximate stresses are recovered using exact stress recovery relationships:

$$\tilde{g}_j(\mathbf{X}) = \tilde{g}_j(\mathbf{X}, \tilde{\mathbf{F}}(\mathbf{Y}(\mathbf{X}))). \tag{9}$$

Note that alternative stress approximations of equal quality can be found in Zhou and Xia (1990) and Zhou and Thomas (1993). Such approximation formulations have been shown to greatly enhance the approximation quality. It is easy to see that this approximation is exact for statically determinate structures since no force redistribution occurs.

Canfield (1990) showed that the quality of the approximation of an eigenvalue can be enhanced by approximating its modal strain energy and modal kinetic energy in the Rayleigh's quotient as intermediate responses:

$$\tilde{\mu}_k(\mathbf{X}) = (\tilde{\omega}_k(\mathbf{X}))^2 = \frac{\tilde{U}_k(\mathbf{Y}(\mathbf{X}))}{\tilde{T}_k(\mathbf{Y}(\mathbf{X}))}. \tag{10}$$

Canfield applied reciprocal approximation to the modal strain energy U_k and linear approximation for the modal kinetic energy T_k.

The general trend for appropriate selection of linear or reciprocal variable space for the approximation of a response type can be observed by studying the behavior of the analysis equations. For example, reciprocal intermediate variables are most suited for the approximation of displacements. However, since a simple separable approximation cannot fully capture the high nonlinearity and complexity of the exact response function, such general rules may not apply to a specific response. Therefore, the choice of the "best" approximation formulation among Eqs. 4–6 could be quite heuristic for an individual response. Thomas (1996) introduced an adaptive approach to selecting the appropriate approximation in the form of Eqs. 4–6 along with the iterative process. This approach has been shown to further improve the efficiency of the optimization process. Note that for shape design variables, no intermediate variables are used in this work.

The advanced approximation techniques summarized herein are implemented in the Altair OptiStruct code for the integrated problem covering sizing, shape, and topology optimization. Note that many approximation approaches that are well suited for other types of optimization problems are not mentioned in this paper. For a review, see the paper by Barthelemy and Haftka (1993).

4 Sensitivity analysis

Discrete sensitivity analysis directly formulated on the basis of the discrete finite element formulation is used. An overview of sensitivity analysis can be found in textbooks

and review papers (see, e.g., Haftka and Adelman 1993; Haftka and Gürdal 1992; Kirsch 1993). For static analysis, responses such as displacements, stresses, and forces can be expressed as a function of the displacement vector $\mathbf{U}$ as follows:

$$R_j(\mathbf{Y}) = \mathbf{Q}_j^T \mathbf{U}. \tag{11}$$

The derivatives of the response can be expressed as:

$$\frac{\partial R_j}{\partial y_i} = \frac{\partial \mathbf{Q}_j^T}{\partial y_i}\mathbf{U} + \mathbf{Q}_j^T \frac{\partial \mathbf{U}}{\partial y_i}\ . \tag{12}$$

From the stiffness equation

$$\mathbf{K}\mathbf{U} = \mathbf{P}, \tag{13}$$

where $\mathbf{K}$ is the stiffness matrix and $\mathbf{P}$ the load vector, the following equation can be derived for the calculation of the displacement sensitivities:

$$\mathbf{K}\frac{\partial \mathbf{U}}{\partial y_i} = \frac{\partial \mathbf{P}}{\partial y_i} - \frac{\partial \mathbf{K}}{\partial y_i}U. \tag{14}$$

In Eq. 14, the vector $\partial \mathbf{U}/\partial y_i$ can be interpreted as the displacement vector corresponding to a load vector $\bar{\mathbf{P}}_i = \frac{\partial \mathbf{P}}{\partial y_i} - \frac{\partial \mathbf{K}}{\partial y_i}\mathbf{U}$, where $\bar{\mathbf{P}}_i$ is termed the pseudoload vector. For N_y intermediate variables, N_y pseudoload vectors need to be solved for each loading case to calculate the derivatives of any number of responses.

Substitution of Eq. 14 into Eq. 12 yields the following expression:

$$\frac{\partial R_j}{\partial y_i} = \frac{\partial \mathbf{Q}_j^T}{\partial y_i}\mathbf{U} + \bar{\mathbf{U}}_j^T \left(\frac{\partial \mathbf{P}}{\partial y_i} - \frac{\partial \mathbf{K}}{\partial y_i}\mathbf{U}\right)\ , \tag{15}$$

with

$$\mathbf{K}\bar{\mathbf{U}}_j = \mathbf{Q}_j. \tag{16}$$

The method using Eq. 15 for sensitivity analysis is called the adjoint method. The vectors $\bar{\mathbf{U}}_j$ and $\mathbf{Q}_j$ are called the adjoint displacement vector and the adjoint load vector, respectively. The solution of one adjoint vector is needed for calculating the derivatives of each response. For N_R responses involved in the approximate problem, the total number of adjoint load vectors is N_R, which is independent of the number of design variables.

It is easy to see that for a specific load case the adjoint method is more efficient than the direct method if N_R related to this load case is smaller than N_y, and vice versa. Both methods are implemented in OptiStruct, and the favorable one is automatically selected according to this rule.

For sensitivity with respect to shape design variables, the so-called semianalytical method is used. In this approach, the derivatives of the stiffness matrix are calculated using central finite differences as follows:

$$\frac{\partial \mathbf{K}}{\partial x_i} = \frac{\mathbf{K}(x_i + \Delta x_i) - \mathbf{K}(x_i - \Delta x_i)}{2\Delta x_i}. \tag{17}$$

It has been shown that very large errors can occur when this method is used. This phenomenon has stimulated intensive research effort in revealing the reasons for the errors and developing methods to eliminate them (see, e.g., Barthelemy and Haftka 1993; Olhoff *et al.* 1993).

5 Iterative scheme

The overall iterative scheme is shown in the flowchart in Fig. 1. For the optimization of the explicit approximate problem, two optimizers are used in OptiStruct. The optimizer CONMIN is an implementation of the method of feasible directions by Vanderplaats (1973), and the optimizer CONLIN is an implementation of the dual method based on convex separable approximations developed by Fleury (1989). Because of the use of intermediate variables for the approximation formulation, the approximate problem involves, in general, functions that are nonconvex and nonseparable. Therefore, an inner iteration loop has to be implemented to solve the approximate problem iteratively using the CONLIN optimizer, as suggested by Zhou (1990) and Zhou and Xia (1989).

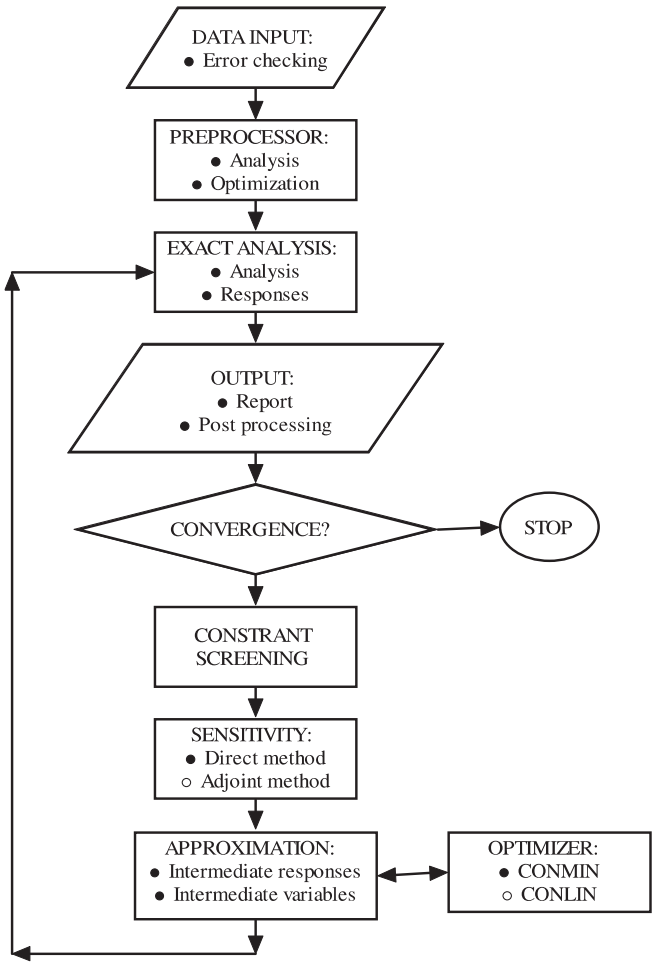

Fig. 1 Flowchart of the optimization process

The method of feasible directions is very robust; however, it is not efficient for problems with a large number of design variables. Since the number of design variables is usually large for design problems involving topology and/or topography optimization (Voth 1999; Altair Engineering 1999), the CONLIN optimizer is selected a priori for such problems. Otherwise, the CONLIN optimizer is only selected if the number of constraints is significantly smaller than the number of design variables. Topography optimization is a special shape optimization tool developed by Voth (1999) for optimizing bead patterns of shell structures. Shape design variables are generated in an automatic fashion using the bead minimum width, draw height, and draw angle defined by the user.

6 Numerical examples

Two numerical examples are presented to illustrate the capabilities of the optimization procedure.

Example 1 – Twist plate optimization: A steel plate of dimension 50×100 mm is fixed at two adjacent corners (short side) and loaded with two equal and opposite out-of-plane forces (of magnitude 1 N) at the other two corners. The Young's modulus E is $200\,000\,\mathrm{N/mm^2}$. The plate is modeled using 5000 uniform, square shell elements of dimension 1×1 mm. The compliance for this loading condition is minimized. Seven optimization studies were conducted.

The first optimization study is a pure shape optimization of the twist plate. The shape design variables are automatically generated by the bead generation capability of OptiStruct (Altair Engineering 1999; Voth 1999). The bead parameters are: bead minimum width 15 mm, draw angle 60°, and draw height 5 mm. The plate thickness is fixed at 1 mm. The optimal shape is shown in Fig. 2. The optimizer successfully reduces the compliance from its initial value of 0.09636 to 0.01314 in 21 iterations. The volume of the plate increases from $5000\,\mathrm{mm^3}$ to $5606\,\mathrm{mm^3}$. However, the compliance has been reduced to only 13.6% of that of the flat plate. In the next six optimization studies, this final volume is imposed as an upper bound constraint.

The second optimization study is a pure topological optimization of the twist plate. The topological design variables are the material densities of the elements in the plate model. The maximum plate thickness is set to 3 mm, and the base plate thickness is zero. Checkerboard control (Altair Engineering 1999) is turned on during the optimization. The optimal topology is shown in Fig. 3. The optimizer reduces the compliance to a final value of 0.01217 in 23 iterations. The upper bound volume constraint is active.

The third optimization study is a small variant of the second in that the base plate thickness during the topology optimization is set to 0.3 units. The optimal topology is shown in Fig. 4. This topology is very similar to the one corresponding to a base plate thickness of zero obtained from the previous study. This is because the optimal load path for the twist plate for this particular loading is clearly determined. The final compliance value is 0.01557 (24 iterations), about 28% higher than the final compliance value from the zero base plate thickness optimization. This is because the rib size in this case is thinner than that obtained in the previous study, owing to less material being available for forming ribs.

The fourth and fifth optimization studies are a combined contour and topology optimization of the twist plate. The base plate thickness is set to zero, and the maximum plate thickness is 3 units. The fifth optimization study has minimum member size control (Zhou *et al.* 1999; Altair Engineering 1999) turned on. The minimum member size is set to 5 units (size of five element widths in this model). Figure 5 shows the final density distribution and contour of the plate corresponding to the fourth optimization study. Figure 6 shows the final density distribution and contour corresponding to the fifth optimization study with minimum member size control. The final compliance values are 0.00778 (30 iterations) and 0.00690 (51 iterations), respectively. Clearly, the integrated topology and contour optimization yields stiffer designs than the pure contour and pure topological optimization studies.

Fig. 2 Contour of the twist plate – pure contour optimization

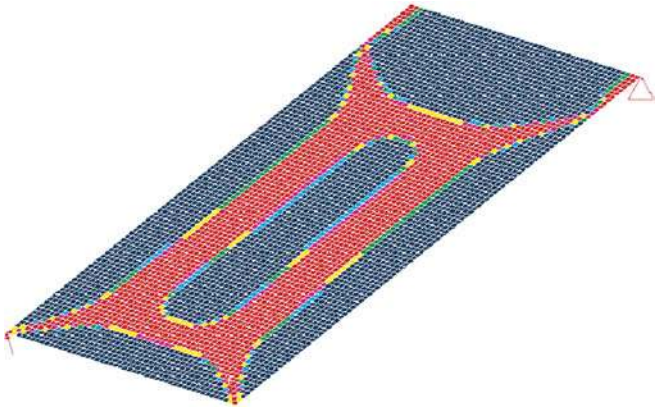

Fig. 3 Density distribution of the twist plate – pure topology optimization (base plate thickness = 0)

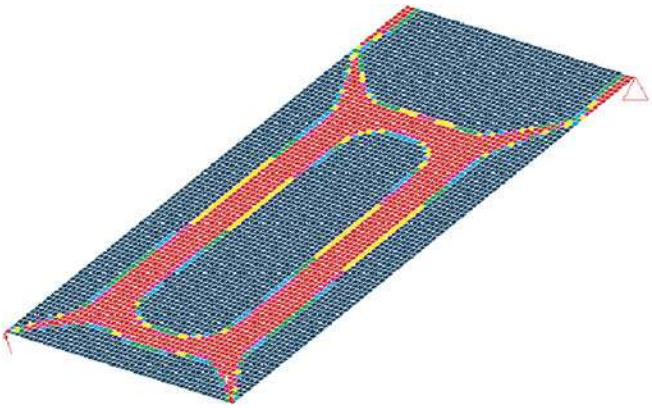

Fig. 4 Density distribution of the twist plate – pure topology optimization (base plate thickness = 0.3 mm)

The minimum member size control takes more iterations to converge but consolidates the rib patterns and eliminates some of the thinner members obtained in the study without this control, thereby improving the stiffness as well as the manufacturability of the final design. Minimum size control does not affect the final contours significantly, as seen from the similarity of Figs. 5 and 6.

The sixth and seventh optimization studies differ from the fourth and the fifth in that the base plate thickness is

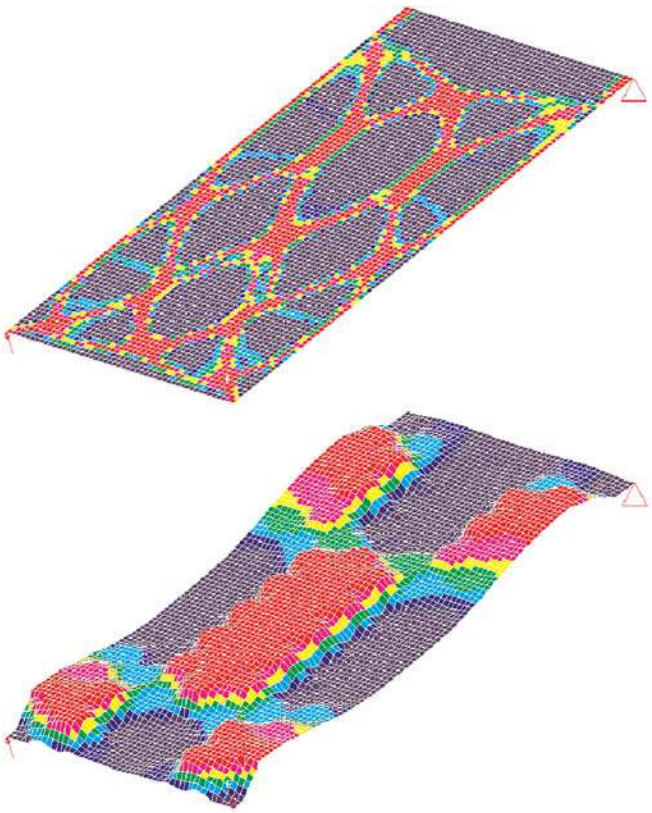

Fig. 5 Density distribution (*top*) and contour (*bottom*) of the twist plate – contour + topology optimization (base plate thickness = 0, no minimum member size control for topology optimization)

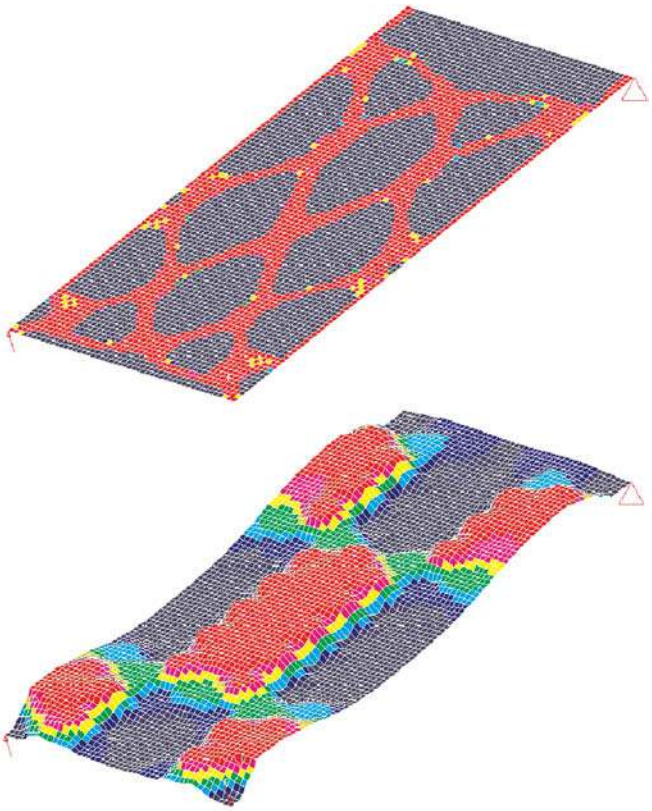

Fig. 6 Density distribution (*top*) and contour (*bottom*) of the twist plate – contour + topology optimization (base plate thickness = 0, with minimum member size control for topology optimization)

set to 0.3 units. Figure 7 shows the final density distribution and contour of the plate corresponding to the sixth optimization study. Figure 8 illustrates the final topology and contour corresponding to the seventh optimization study with minimum member control. The final compliance values are 0.00862 (24 iterations) and 0.00847 (62 iterations), respectively. Several important observations must be made from these results. The final contours obtained from these two studies (Figs. 7 and 8), though similar to each other, are quite different from those obtained in the previous two studies (Figs. 5 and 6). Indeed, the final contours are closer to that obtained in the first study (Fig. 2). This difference in contours is attributed to the structural stiffness obtained from the presence of the base plate. The density distributions (Figs. 7 and 8) are quite similar, unlike the previous two studies (Figs. 5 and 6). This is because the base plate takes up about one third of the available material (based on the upper bound volume constraint). Because of the limited material available, thinner ribs are not formed and minimum member control does not change the topology significantly.

Example 2 – Oil pan optimization: A steel oil pan, used to collect the engine oil from an automobile, is designed for minimum volume of the structure. Lower bound constraints of 10 Hz, 10 Hz, 12 Hz, and 15 Hz are imposed on the first four eigenfrequencies, respectively, for the purpose of noise reduction. The pan

is 200 mm wide and 500 mm long and has two levels of depths, 75 mm and 150 mm, respectively. The Young's modulus E is 200 000 N/mm^2, and the density is 7.87×10^{-6} kg/mm^3. The oil pan is modeled using 2392 shell elements and is fixed at eight points along the lip of the pan (Fig. 9). The lip has a thickness of 0.7 mm and is defined as nondesign domain. The initial design has a shell thickness of 0.18 mm and a volume of 56 434.6 mm^3. The first four eigenfrequencies of the initial design are 1.48 Hz, 1.499 Hz, 1.631 Hz, and 1.973 Hz, respectively, which implies that the frequency constraints are severely violated in the initial design. Six optimization studies were conducted.

The first optimization study is a pure contour shape optimization. The bead parameters are: bead minimum width 125 mm, draw angle 60°, and draw height 10 mm (Altair Engineering 1999). The plate thickness is fixed at 0.18 mm. The iterative process converged after 77 iterations. The final contour shape is shown in Fig. 10. The four first eigenfrequencies of the final design are 10.00 Hz, 10.25 Hz, 12.09 Hz, and 14.483 Hz, respectively. Only the fourth constraint has a 1.1% constraint violation. The volume of the final design is 55 688.4 mm^3. The initial design has highly violated constraints, and much of the optimization effort goes into recovering these violated constraints.

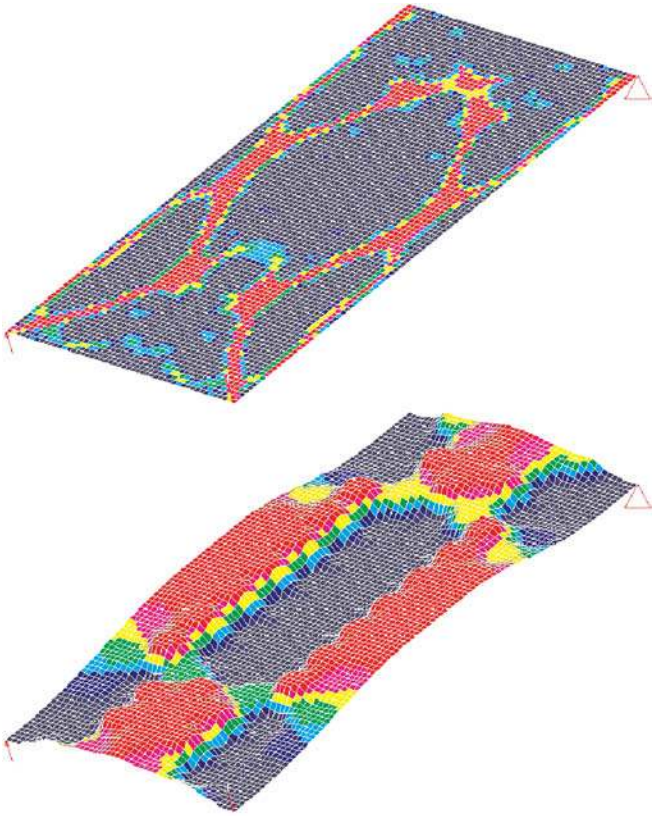

Fig. 7 Density distribution (*top*) and contour (*bottom*) of the twist plate – contour + topology optimization (base plate thickness = 0.3 mm, no minimum member size control for topology optimization)

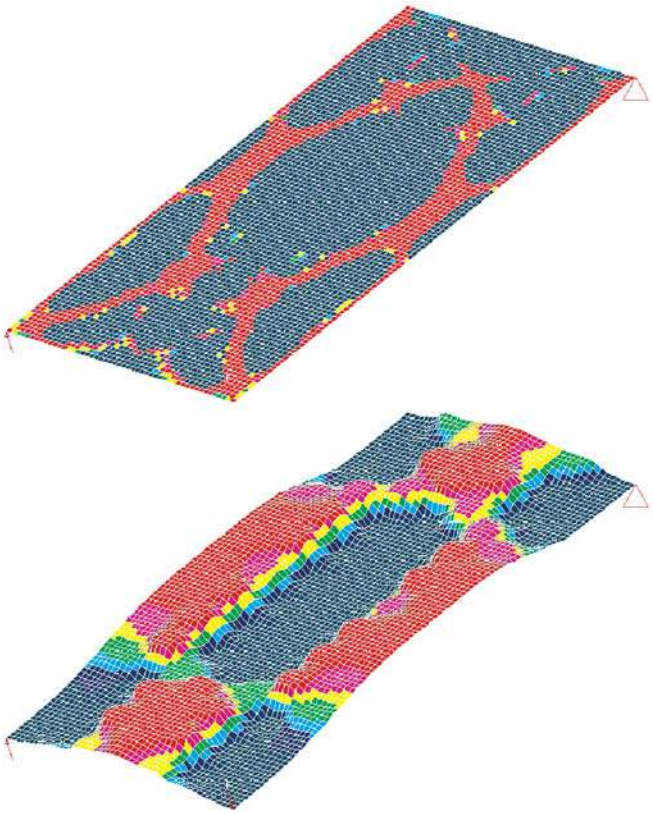

Fig. 8 Density distribution (*top*) and contour (*bottom*) of the twist plate – contour + topology optimization (base plate thickness = 0.3 mm, no minimum member size control for topology optimization)

The second optimization study is a pure topology optimization. The maximum plate thickness is set to 3.0 mm, and the base plate thickness is 0.1 mm. The iterative process converged after 35 iterations. The density distribution of the final design is shown in Fig. 11. The four first eigenfrequencies of the final design are 9.99 Hz, 10.01 Hz, 12.26 Hz, and 14.98 Hz, respectively. Constraints 1 and 4 are marginally violated (0.1% each). The volume of the final design is 125 373 mm^3.

The third optimization study is a combined contour and sizing optimization of the oil pan. The plate thick-

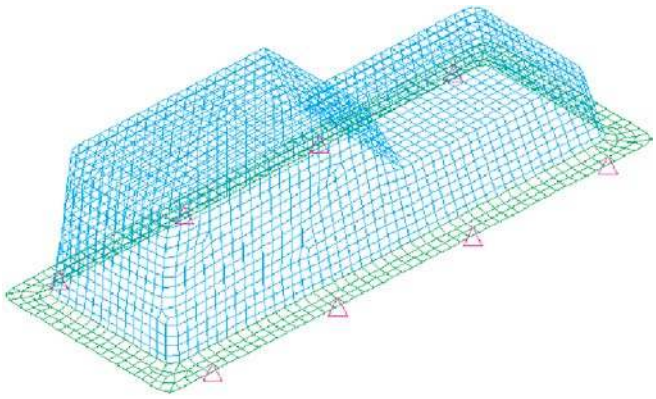

Fig. 9 Finite element model of the oil pan

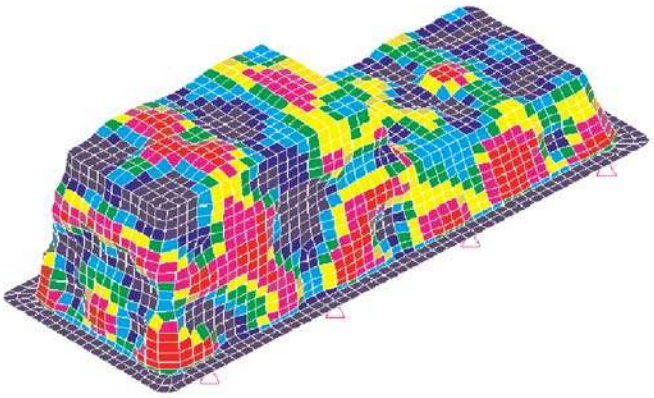

Fig. 10 Contour shape of the oil pan – pure contour optimization

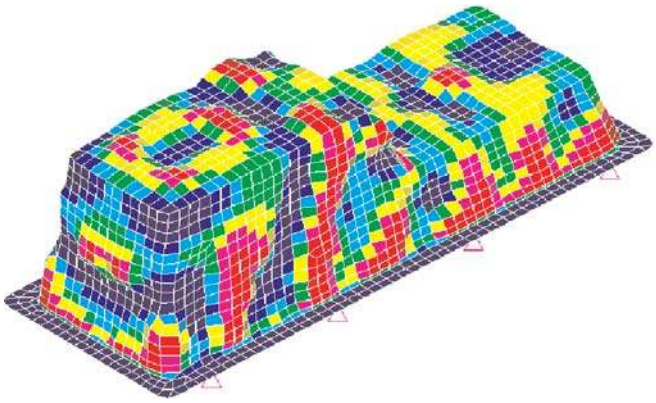

Fig. 12 Contour shape of the oil pan – contour + sizing optimization

ness of the shell elements in the design domain is used as the sizing variable. Its initial value is 0.18 mm, and its lower and upper bounds are set to 0.1 mm and 2.0 mm, respectively. The bead parameters are the same as those used in the first study. The iterative process converged after 68 iterations. The final thickness is 0.1424 mm. The final contour shape is shown in Fig. 12. The four first eigenfrequencies of the final design are 10.46 Hz, 10.53 Hz, 12.01 Hz, and 14.95 Hz, respectively. Only the fourth frequency constraint is violated by 0.3%. The volume of the final design is 48 149.1 mm^3. This particular case study illustrates the advantage of having the freedom to integrate sizing and shape variables in the optimization loop over a pure shape optimization.

The fourth optimization study is a combination of sizing and topology optimization. As in the third study, the plate thickness of the elements in the design domain is used as the sizing design variable. Its initial value is 0.18 mm, and its lower and upper bounds are set to 0.1 mm and 3.0 mm, respectively. The iterative process converged after 36 iterations. The density distribution of the final design is shown in Fig. 13. The first four eigenfrequencies of the final design are 9.98 Hz, 10.02 Hz, 12.34 Hz, and 14.93 Hz, respectively. The first constraint and the fourth constraint are marginally violated (0.2% and 0.5%, respectively). The volume of the structure is 128 280 mm^3. Note that this design is somewhat similar to the design from the second study.

The fifth optimization study is a combination of the contour optimization and the topology optimization described in studies 1 and 2, respectively. The iterative process converged after 68 iterations. The density distribution and the contour shape of the final design are shown in Fig. 14. The four first eigenfrequencies of the final design are 10.91 Hz, 11.32 Hz, 12.99 Hz, and 14.98 Hz, respectively. Except for the fourth frequency constraint, which is marginally violated (0.1%), all the constraints are well satisfied. The volume of the final design is 45 080 mm^3.

The sixth optimization study is combination of sizing, contour, and topology optimization. The iterative process converged after 80 iterations. The density and contour distributions are shown in Fig. 15. The first four eigenfrequencies of the final design are 11.45 Hz, 11.47 Hz, 13.87 Hz, and 14.99 Hz, respectively. All constraints are successfully recovered with only the fourth constraint having a marginal 0.1% constraint violation. The volume of the final design is 57 078.3 mm^3, and the final plate thickness is 0.543 mm.

A comparison of the six studies reveals that the combination of contour and topology optimization gave the

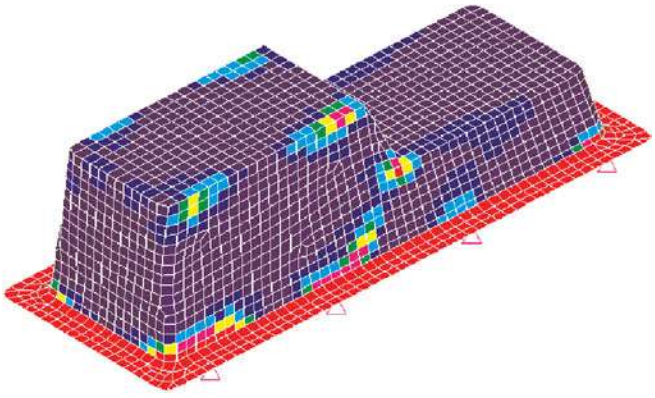

Fig. 11 Density distribution of the oil pan – pure topology optimization

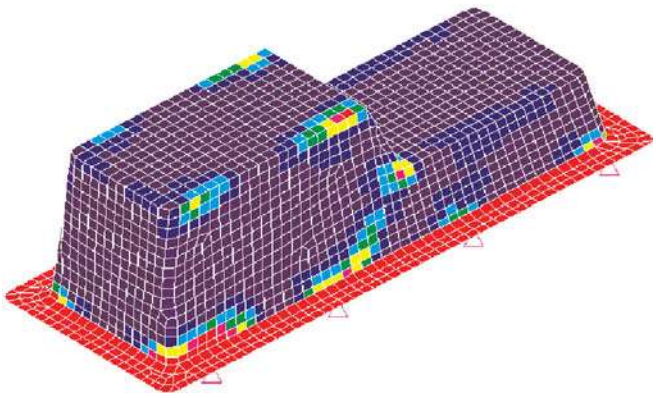

Fig. 13 Density distribution of the oil pan – topology + sizing optimization

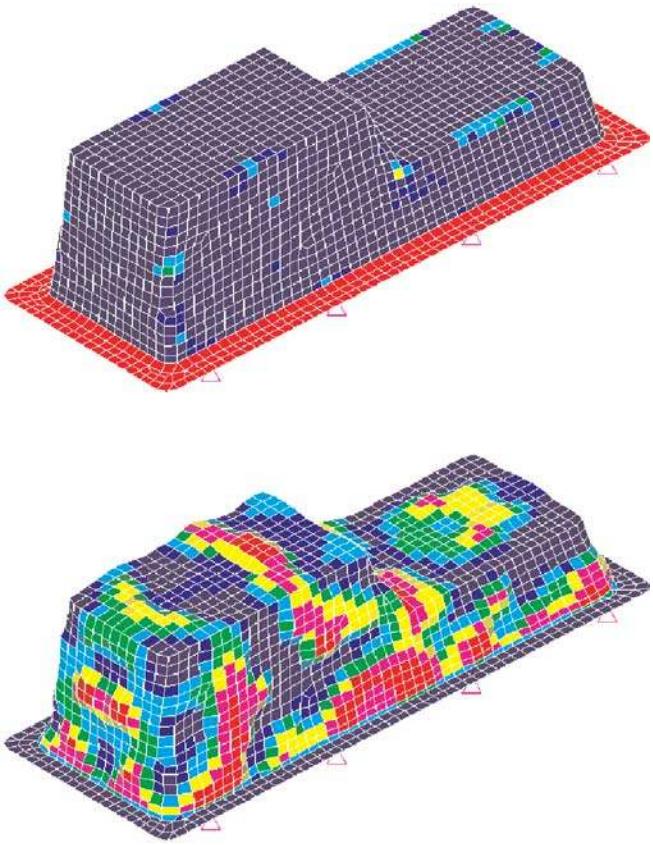

Fig. 14 Density distribution (*top*) and contour shape (*bottom*) of the oil pan – contour + topology optimization

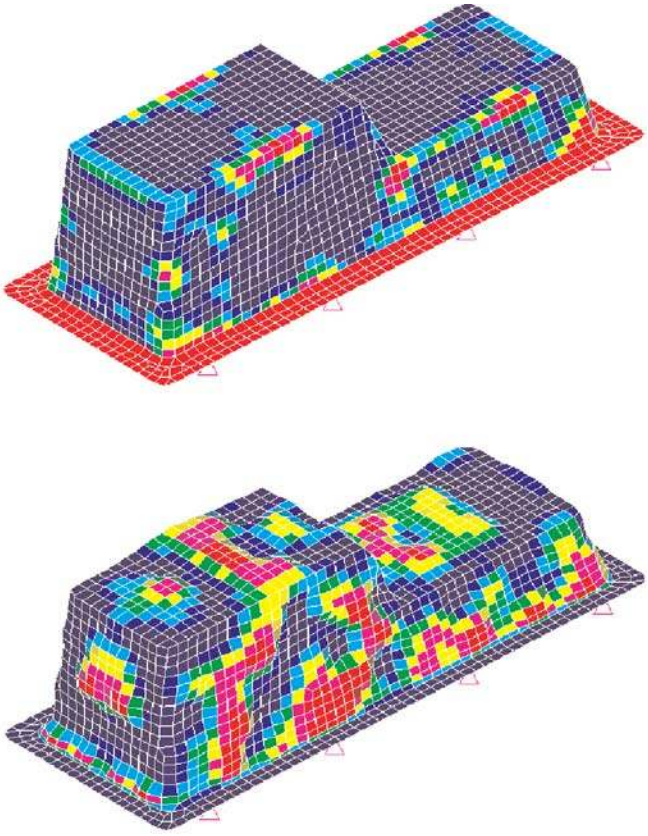

Fig. 15 Density distribution (*top*) and contour shape (*bottom*) of the oil pan – contour + topology optimization

best result. Although the combination of sizing, contour, and topology optimization represents the maximum design freedom, its final volume is higher than the study without the sizing variable. The reason is that, in general, there exist a large number of local optima for such complicated problem formulations. Since the gradient-based optimization algorithms could only converge to a local optimum, the final results should always be assessed with a critical view.

7 Concluding remarks

The integration of sizing, shape, and topology optimization in a single iterative process has been studied in this work. This unique capability has been created within the commercial code Altair OptiStruct during the process of extending it into a general structural optimization tool that provides sizing, shape, and topology optimization capabilities. Emphasis has been placed on integrating state-of-the-art techniques that enhance the overall efficiency of the optimization process. Advanced approximation techniques, which have been discussed in detail, play a central role in this regard. The feasibility of combining topology optimization with sizing and shape optimization has been studied with numerical examples. Promising results have been obtained for the examples considered.

The ability to combine different types of optimization variables provides increased freedom for concept study. However, caution needs to be exercised when different types of design variables are considered simultaneously. Since the freedom of design choice increases under the integrated treatment of different types of design variables, the feasible domain of the design space may become highly nonconvex, resulting in the existence of a large number of local optima. Therefore, the resulting design should be assessed with a critical view. In general, experimenting with different combinations of design variables could help understand the behavior of a specific design problem.

Note also that a user-friendly graphic interface for OptiStruct has been developed with Altair HyperMesh (Altair Engineering 2000). Within this modeling environment, the user can interactively set up the details of the optimization problem such as design variable selection, objective function, and design constraint definitions.

References

Allaire, G.; Kohn, R.V. 1993: Topology optimization and optimal shape design using homogenization. In: Bendsøe, M.P.; Mota Soares, C.A. (eds.) *Topology design of structures*, 207–218

Altair HyperMesh 2000: Users manual. Altair Engineering, Inc., Troy, MI

Altair OptiStruct 1999: Users manual. Altair Engineering, Inc., Troy, MI

ANSYS 1999: Users manual. ANSYS, Inc., Houston, PA

Barthelemy, J.M.; Haftka, R.T. 1993: Recent advances in approximation concepts for optimum structural design. *Struct. Optim.* **12**, 129–144

Bendsøe, M. 1989: Optimum shape design as a material distribution problem. *Struct. Optim.* **1**, 193–202

Bendsøe, M. 1995: *Optimization of structural topology, shape and material.* Berlin: Springer-Verlag

Bendsøe, M.; Kikuchi, N. 1988: Generating optimal topologies in optimal design using a homogenization method. *Comp. Meth. Appl. Mech. Engrg.* **71**, 197–224

Canfield, R.A. 1990: High quality approximation of eigenvalues in structural optimization. *AIAA J.* **28**, 1143–1149

Chang, K.H.; Choi, K.K. 1992: A geometry-based parameterization method for shape design of elastic solids. *Mech. Struct. & Mach.* **20**, 215–252

Ding, Y. 1986: Shape optimization of structures – a literature survey. *Comp. Struct.* **24**, 985–1004

Fluery, C. 1989: CONLIN: an efficient dual optimizer based on convex approximation concepts. *Struct. Optim.* **1**, 81–89

Fleury, C.; Braibant, V. 1986: Structural optimization: a new dual method using mixed variables. *Int. J. Num. Meth. Engrg.* **23**, 409–428

GENESIS 1999: Users manual. VMA Engineering, Inc., Colorado Springs, CO

Haftka, R.T.; Adelman, H.M. 1993: Sensitivity of discrete systems. In: Rozvany, G.I.N. (ed.) Optimization of Large Structural Systems, Dordrecht: Kluwer Academic Publishers, pp. 289–212

Haftka, R.T.; Grandhi, R.V. 1986: Structural shape optimization – a survey. *Comp. Meth. Appl. Mech. Engrg.* **57**, 91–106

Haftka, R.T.; Gürdal, Z. 1992: *Elements of structural optimization.* Dordrecht: Kluwer Acad. Publ.

Haftka, R.T.; Starnes, J.H. 1976: Application of a quadratic extended interior penalty function for structural optimization. *AIAA J.* **14**, 718–724

Kikuchi, N.; Chung, K.Y.; Torigaki, T.; Taylor, E. 1986: Adaptive finite element methods for shape optimization. *Comp. Meth. Appl. Mech. Engrg.* **57**, 67–89

Kirsch, U. 1993: *Structural optimization: fundamentals and applications.* Berlin: Springer-Verlag

MSC/NASTRAN 1999: Users manual. MSC Software, Inc., Los Angeles, CA

Olhoff, N.; Rasmussen, J.; Lund, E. 1993: Method of "exact" numerical differentiation for error elimination in finite element based semi-analytical sensitivity analysis. *Mech. Struct. Mach.* 21, 1–66

Olhoff, N.; Rønholt, E.; Scheel, J. 1998: Topology optimization of plate-like structures using 3-D elasticity and optimum 3-D microstructures. *Proc. 7th AIAA/USAF/NASA/ISSMO Symposium on Multidisciplinary Analysis and Optimization*, St. Louis, Missouri, 1853–1863

Rozvany, G.I.N.; Bendsøe, M.; Kirsch, U. 1995: Layout optimization of structures. *Appl. Mech. Rev.* **48**, 41–119

Schleupen, A.; Maute, K.; Ramm, E. 1995: Adaptive FE-procedures in shape optimization. *Struct. Optim.* **19**, 282–302

Schmit, L.A. 1981: Structural synthesis – its genesis and development. *AIAA J.* **19**, 1249–1263

Schmit, L.A.; Farshi, B. 1974: Some approximation concepts for structural synthesis. *AIAA J.*, **12**, 692–699

Schramm, U.; Pilkey, W.D. 1993: The coupling of geometric descriptions and finite elements using NURBs – a study in shape optimization. *Finite Elements in Analysis and Design*, **15**, 11–34

Sigmund, O.; Petersson, J. 1998: Numerical instabilities in topology optimization: A survey on procedures dealing with checkerboards, mesh-dependencies and local minima. *Struct. Optim.* **16**, 68–75

Thomas, H.L. 1996: Optimization of structures designed using nonlinear FEM analysis. *Proc. 7th AIAA/ASME/ASCE/AHS/ASC 37th Structures, Structural Dynamics and materials conference*, April, Salt Lake City, UT

Vanderplaats, G.N. 1973: CONMIN – a Fortran program for constrained function minimization: user's manual. NASA TM X-62282

Vanderplaats, G.N. 1982: Structural optimization – past, present and future. *AIAA J.* **20**, 992–1000

Vanderplaats, G.N.; Salajegheh, E. 1989: A new approximation method for stress constraints in structural synthesis. *AIAA J.* **27**, 252–358

Vanderplaats, G.N.; Thomas, H.L. 1993: An improved approximation for stress constraints in plate structures. *Struct. Optim.* **6**, 1–6

Voth, B. 1999: Using automatically generated shape variables to optimize stamped plates. Technical Memorandum, Altair Engineering, Inc., Troy, MI

Yang, R.J.; Lee, A.; McGeen, D.T. 1992: Application of basis function concept to practical shape optimization problems. *Struct. Optim.* **5**, 55–63

Zhou, M. 1989: Geometrical optimization of trusses by a two-level approximation concept. *Struct. Optim.* **1**, 235–240

Zhou, M.; Rozvany, G.I.N. 1991: The COC algorithm, Part II: topological, geometry and generalized shape optimization. *Comp. Meth. Appl. Mech. Engrg.* **89**, 197–224

Zhou, M.; Shyy, Y.K.; Thomas, H.L. 1999: Checkerboard and Minimum Member Size Control in Topology Optimization. *Struct. Multidisc. Optim.* **21**, 152–158

Zhou, M.; Thomas, H.L. 1993: Alternative approximation for stresses in plate structures. *AIAA J.* **31**, 2169–2174

Zhou, M.; Xia, R.W. 1990: Two-level approximation concept in structural synthesis. *Int. J. Num. Meth. Engrg.* **29**, 1681–1699